Local Excitation, Scattering, and Interference of Surface Plasmons

B. Hecht,[1] H. Bielefeldt,[1] L. Novotny,[2] Y. Inouye,[1,*] and D. W. Pohl[1,†]

[1]*IBM Research Division, Zurich Research Laboratory, CH-8803 Rüschlikon, Switzerland*

[2]*Swiss Federal Institute of Technology, Eidgenössische Technische Hochschule Zürich, CH-8092 Zurich, Switzerland*

(Received 14 December 1995; revised manuscript received 29 March 1996)

The optical probe of a scanning near-field optical microscope is shown to act as a *point source of surface plasmon* (SP) *polaritons* on gold and silver films. Plasmon excitation manifests itself by emission of light in the direction of the SP resonance angle, originating from an area with the shape of a dipole radiation pattern whose extension is given by the SP decay length. Interaction with selected, individual surface inhomogeneities gives rise to characteristic modifications of the emitted radiation, which provide detailed information about SP scattering, reflection, and interference phenomena. [S0031-9007(96)01079-4]

PACS numbers: 78.66.Bz, 42.25.Hz, 42.30.Va, 71.36.+c

Surface plasmons (SP) in thin metallic films have been studied extensively [1]. Their properties with regard to such parameters as material constants and film thickness are well understood. Little is known, however, about the effects of individual perturbations of film homogeneity, although the measurable SP properties are strongly influenced by the presence of adsorbed particles, grain boundaries, growth hillocks, etc.

The lack of detailed information is primarily a consequence of classical experimental techniques [2,3], which produce *extended-plane* SP waves and detect SP effects *averaged over macroscopic-sized* areas. More recently, scanned probe techniques have been used to monitor locally the intensity of extended-plane SP waves [4–11] generated by means of the well-known Kretschmann technique [3].

Our experimental investigations were inspired by the idea of generating an *SP point source* that can selectively irradiate a structure of interest on a metal surface. A source of this kind would allow SP interactions to be studied with the individual, selected surface structures unperturbed by the mess of scattered wavelets produced by extended waves. The optical probe of an emission-mode aperture scanning near-field optical microscope (SNOM) [12–14] appears predestined for this purpose: The light at its apex is confined to a spot with a diameter much smaller than the wavelength of the corresponding SP. Its Fourier transform hence comprises components with finite amplitude at k_{SP}, which is the wave vector of the SP exceeding that of freely propagating light (k_0) at a given excitation frequency. Furthermore, the positioning capability of the SNOM allows SP interactions with purposefully selected features to be studied in a systematic way. It will be shown that, in addition, the direction of SP emission can be chosen at will by adjusting the polarization of the light source appropriately.

First observations made with such an SP point source will be presented in this Letter. A transmission SNOM with a specific light detection scheme, a "TNOM" [15], was used for this purpose. In addition to the classically refracted, *allowed* light, the radiation emitted into the classically *forbidden* directions is also detected in the TNOM configuration. These two regimes are separated by the critical angle $\theta_c = \arcsin(1/n) = 41.12°$ (n is the refractive index of the glass substrate). The capability to detect forbidden light is instrumental for the investigation of SP resonance radiation. The latter is emitted from a planar metal film into the substrate at an angle of $\theta_{SP} = \arcsin(k_{SP}/nk_0) > \theta_c$ as a consequence of the phase-matching requirement [1].

The optical probes in our experiments were aluminum-coated glass fiber tips with a 50–100 nm radius aperture [Fig. 1(a)]. The light source was either a HeNe or an Ar^+ laser, i.e., $\lambda = 633$ or 514 nm. The illumination scheme

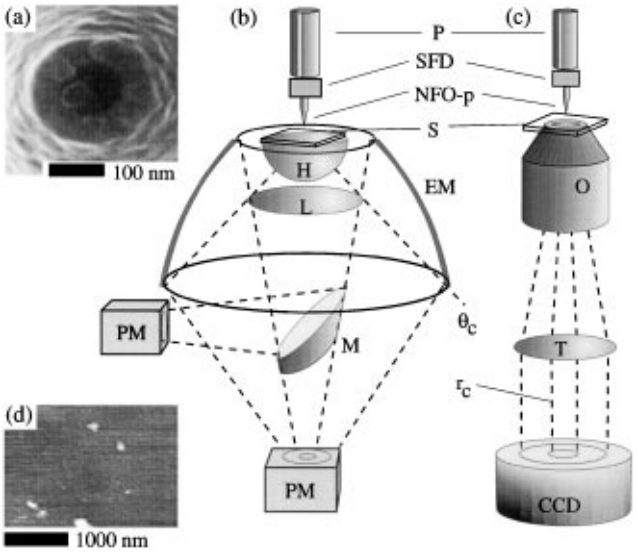

FIG. 1. TNOM: (a) Scanning electron microscopy image of the apex of a typical aperture NFO fiber probe. (b) Original setup, from [15]. P: tube piezo, SFD: shear force detector, NFO-p: near-field optical probe, M: mirror. (c) Setup for the investigation of spatial and angular distributions of the transmitted light. (d) Typical topography of a silver film used as sample (roughness ≈1 nm, height of protrusions ≈40 nm).

and the two detection arrangements used are shown in Figs. 1(b) and 1(c).

The detector configuration in Fig. 1(b) is described in detail in Ref. [15]. Forbidden and allowed light from the sample film (S), after passing through a glass hemisphere (H), are directed onto the two photomultipliers (PM) by an elliptical mirror (EM) and an objective lens (L), respectively. This setup was used primarily to generate scan images.

The detection setup in Fig. 1(c) is designed for direct observation of SP propagation and angular distribution of the emitted resonance radiation. For this purpose, the sample is placed on an inverted microscope (Zeiss Axiovert 10) equipped with a 40×, N.A. = 1.3 immersion objective (O) and a charge coupled device camera. Besides the allowed light, restricted to a circle with radius r_c, the objective also captures the forbidden radiation with divergence up to 60°.

The samples were silver and gold films of 60 ± 20 nm thickness, evaporated onto thin cover slides. All samples were checked for reflectivity quenching at θ_{SP} [3]. A typical topographic (shear force) image of such a film is depicted in Fig. 1(d). The flatness of the film surface is interrupted only by a number of small protrusions (bright spots), which might be growth hillocks of the film or irregularities of the glass substrate.

First, the angular distributions of the radiation transmitted by gold and silver films were examined. This was possible with both setups after the minor modifications of replacing the elliptical mirror and objective lens by a Polaroid cassette in Fig. 1(b), and defocusing the objective in Fig. 1(c) such that the radiation from the sample leaves the tubus lens (T) as a collimated beam.

Without a metal film and with the near-field optical (NFO) probe in retracted position, the transmitted light is restricted to a sharply defined circular area, its radius corresponding to θ_c as expected. When the NFO probe is at operating distance, the illumination extends over a considerably larger area with diffuse borders, owing to the presence of forbidden light.

The emission patterns recorded for gold and silver films are radically different. For unpolarized light, a sharply defined, thin ring is observed [Fig. 2(a), 515 nm, silver], which breaks up into a pair of crescents when linearly polarized light is used for excitation [Fig. 2(b), 633 nm, gold] [16]. The radii correspond to $\theta = 44.3°$ and 43.8°, which can be readily identified as the respective SP resonance angles θ_{SP} [1].

The crescent shape in Fig. 2(b) and its orientation, i.e., along the direction of polarization, are further evidence of SP generation: As a mainly longitudinal, compressional electron density wave, the SP propagates only in the direction of the electric field. In addition, the larger width of the crescents compared to that of the ring supports our assignment, as the gold SP is damped more strongly than the silver SP.

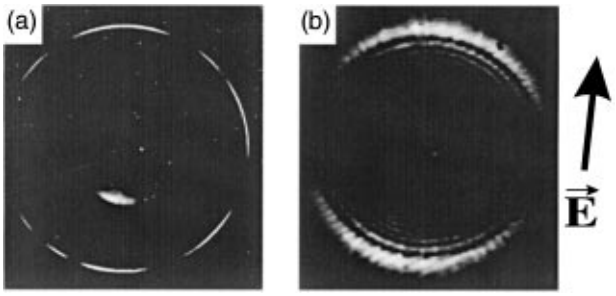

FIG. 2. Angular distribution of transmitted radiation: (a) silver film, $\lambda = 514$ nm, elliptic polarization, detection scheme of Fig. 1(b) (with modifications; see text); (b) gold film, $\lambda = 633$ nm, linear polarization along $\vec{E}$, detection scheme of Fig. 1(c).

Film thickness was chosen such that the film appeared almost opaque upon visual inspection. In fact, practically no light was transmitted when the NFO probe was far enough away from the film surface. The signal grew exponentially during approach. Its decay constant equaled that of an evanescent wave created by total reflection of a wave incident at θ_{SP}. The maximum signal was measured about 30 nm away from contact. At smaller distances, the intensity of the resonant radiation decreased abruptly, ending at a (20–30)% lower value at shear force contact. The decrease is caused by the influence of the metal-coated NFO probe on the propagation of the SP, an assumption supported by numerical simulation results obtained with methods described in previous publications [17].

The *path of SP propagation* becomes visible in the detection scheme in Fig. 1(c) when the objective is focused properly at the metal-film/glass interface. The images obtained map the spatial distribution of SP intensity, as each point of the interface emits resonance radiation in proportion to its SP excitation.

Figures 3(a) and 3(b) reproduce two frames from a video sequence [16] taken while raster scanning a 3μm × 3μm area of a silver film. Two extended lobes are seen to shine up in each of the images. They actually appear only when the NFO probe is at operating distance, in contrast to the bright central spot produced by directly transmitted radiation from the NFO probe (to localize the tip through the objective, a smaller film thickness than in the previous experiments was chosen). The spot is diffraction limited in size but, owing to overexposure, appears to have a diameter of 4 μm.

The two SP lobes are oriented along the direction of polarization of the incident light, consistent with Fig. 2(b). A cut through the intensity distribution along the main axis, averaged over five scan lines in Fig. 3(a), is shown in Fig. 3(c). The lateral variation of the SP intensity roughly fits by an

$$I_{SP} \propto (e^{-\rho/l_{SP}}/\rho)\cos^2\varphi \qquad (1)$$

dependence, where ρ and φ are polar coordinates. This behavior is characteristic for damped radiation from a

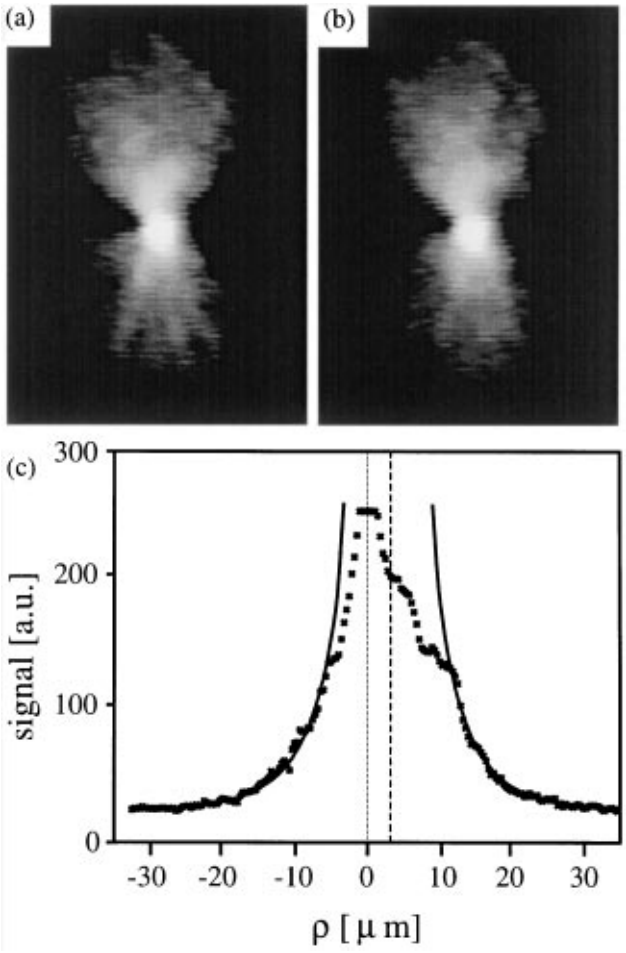

FIG. 3. Maps of spatial distribution and strength of SP on a silver film, $\lambda = 633$ nm [setup of Fig. 1(c), microscope focused to film/glass interface]. (a), (b) 50 μm $\times$ 70 μm-sized frames from a video sequence [16], corresponding to two positions of the NFO probe separated ≈ 1 μm along a scan line of Fig. 1(d). (c) Data points: Cross section through the lobe intensity profile along the main symmetry axis; line: $e^{-\rho/l_{SP}}/\rho$ function fitted by the wings of the profile.

dipole in two dimensions [18]. The resulting decay constant $l_{SP} = 8 \pm 2$ μm is in fair agreement with literature data (9–13 μm) [19,20]. To obtain a decent fit, the center of the fit function depicted in Fig. 3(c) together with the experimental data had to be displaced by about 3 μm with respect to the bright spot. The origin of the displacement is not yet understood. It remained constant during scanning, which could indicate an asymmetry of the aperture and/or the metal coating forming its rim.

The intensity distribution within the lobes shows considerable fine structure, frequently in the shape of "fingers" and abrupt steps. During scanning, the bright stripes of the fingers and the dark ones in between drift through the lobes in a systematic manner, resembling the beams emitted by a rotating mirror beacon. The variations are obvious from a comparison of Figs. 3(a) and 3(b), which are taken from two positions of the same scan line about 1 μm apart. The assumption that the protrusions (bright spots) in Fig. 1(d) block, scatter, and reflect the SP wave at the NFO probe, i.e., as the SP source passes, is close at hand.

The interaction of the SP point source with the irregularities of a silver film turned out to cause peculiar (quasi-) interference effects in NFO images of gold and silver films. Figure 4 shows the results obtained with a Ag film of the type used for Fig. 2(a). The shear force image [Fig. 4(a)] depicts a surface quite similar to that in Fig. 1(d): It is flat within about 1 nm, except for a few protrusions, 50–300 nm in diameter and <40 nm in height.

In the "forbidden" light image, Fig. 4(b), intensity fringes surround protrusions A and B as concentric rings. The amplitude of modulation can be up to 10% of the average signal level. The azimuthal variation of the amplitude corresponds to the direction of polarization of the probe light. The period of undulation is 240 ± 5 nm, i.e., exactly one-half of λ_{SP}. The undulations hence must be caused by interference effects between incident SP and scattered secondary SP waves emerging from the protrusions.

It should be emphasized, however, that the observed fringes cannot represent a true interference pattern, as each pixel of the scan image represents an average over the radiation from an area of about 200 μm^2 (cf. Fig. 3). Hence, variations in the intensity with position cannot be expected to correlate markedly with the local intensity of the SP excitation. Instead, the undulations indicate an influence of the scattered SPs on the overall excitation of and radiation from the plasmon field. Although this mechanism is not yet well understood, the undulation amplitude is obviously proportional to the secondary SP intensity and thus is a measure of the SP/SP scattering efficiency of a given scattering center.

In the "allowed" light image, Fig. 4(c), the most intriguing feature is a set of hyperbolic fringes near the prominent protrusion A. They can be fitted over a sizable area to the family of confocal hyperbolas with foci at A and B and a separation of $\lambda_{SP}/2$ on the A-B axis. The formation of hyperbolas means that the *difference* in distance between the NFO probe and the two scattering centers, modulo $\lambda_{SP}/2$, is the dominant parameter in the allowed image. It follows that in allowed light we observe

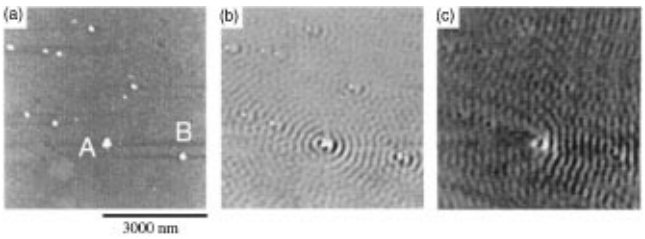

FIG. 4. TNOM scan images of 60 ± 20 nm silver film, 256×256 pixels, 5 ms/pixel scan rate, setup of Fig. 1(b): (a) shear force signal/topography, (b) forbidden, and (c) allowed light ($\lambda = 514$ nm).

the interference between the *light* waves radiated from two different scattering centers into the glass substrates, i.e., out of the film.

In summary, an SP wave with (two-dimensional) dipole radiation characteristics emerges from the NFO probe when the latter is positioned in close proximity to a gold or silver film. The interaction of the SP with individual, nanometer-sized film structures manifests itself in the intensity distribution of the emission lobes and of the NFO scan images. This may open new perspectives for SP spectroscopy and scattering studies on the basis of specific, local experiments.

The authors thank G. Eggers, Ch. Hafner, and H. Heinzelmann for help and discussions. This work was supported in part by the SPP *OPTIQUE* of the board of the Swiss Federal Institutes of Technology and by the European program *Human Capital and Mobility*.

*On leave from Osaka University, Suita, Osaka 565, Japan.
†Electronic address: DP@ZURICH.IBM.COM

[1] H. Raether, in *Surface Plasmons on Smooth and Rough Surfaces and on Gratings*, Springer Tracts in Modern Physics Vol. 111 (Springer-Verlag, Berlin, Heidelberg, 1988).
[2] A. Otto, Z. Phys. **216**, 398 (1968).
[3] E. Kretschmann, Z. Phys. **241**, 313 (1971).
[4] M. Specht, J. D. Pedarnig, W. M. Heckl, and T. W. Hänsch, Phys. Rev. Lett. **68**, 476 (1992).
[5] M. Rücker, W. Knoll, and J. Rabe, J. Appl. Phys. **72**, 5027 (1992).
[6] O. Marti *et al.,* Opt. Commun. **96**, 225 (1993).
[7] P. Dawson, F. de Fornel, and J.-P. Goudonnet, Phys. Rev. Lett. **72**, 2927 (1994).
[8] R. B. G. de Hollander, N. F. van Hulst, and R. P. H. Kooyman, Ultramicroscopy **57**, 263 (1995).
[9] D. P. Tsai *et al.,* Phys. Rev. Lett. **72**, 4149 (1994).
[10] S. I. Bozhevolnyi, B. Vohnsen, I. Smolyaninov, and A. V. Zayats, Opt. Commun. **117**, 417 (1995).
[11] Y.-K. Kim *et al.,* Appl. Phys. Lett. **66**, 3407 (1995).
[12] D. Pohl, W. Denk, and M. Lanz, Appl. Phys. Lett. **44**, 651 (1984).
[13] E. Betzig *et al.,* Science **251**, 1468 (1991).
[14] D. Pohl, in *Scanning Tunneling Microscopy II,* edited by R. Wiesendanger and H.-J. Güntherodt, Springer Series in Surface Science Vol. 28 (Springer-Verlag, Berlin, Heidelberg, 1992), pp. 233–271.
[15] B. Hecht, D. Pohl, H. Heinzelmann, and L. Novotny, Ultramicroscopy **61**, 99 (1995).
[16] An unedited short video sequence showing the formation of crescent and lobes during approach as well as the lobe pattern during during scanning can be made available upon request.
[17] L. Novotny and D. Pohl, in *Photons and Local Probes*, edited by O. Marti and R. Möller, NATO ASI Series E: Applied Sciences Vol. 300 (Kluwer, Dordrecht, 1995), pp. 21–33.
[18] H. von Hörschelmann, Jahrbuch der drahtlosen Telegraphie **60**, 15 (1912).
[19] M. van Exter and A. Lagendijk, Phys. Rev. Lett. **60**, 49 (1988).
[20] N. Kroo *et al.,* Europhys. Lett. **15**, 289 (1991).